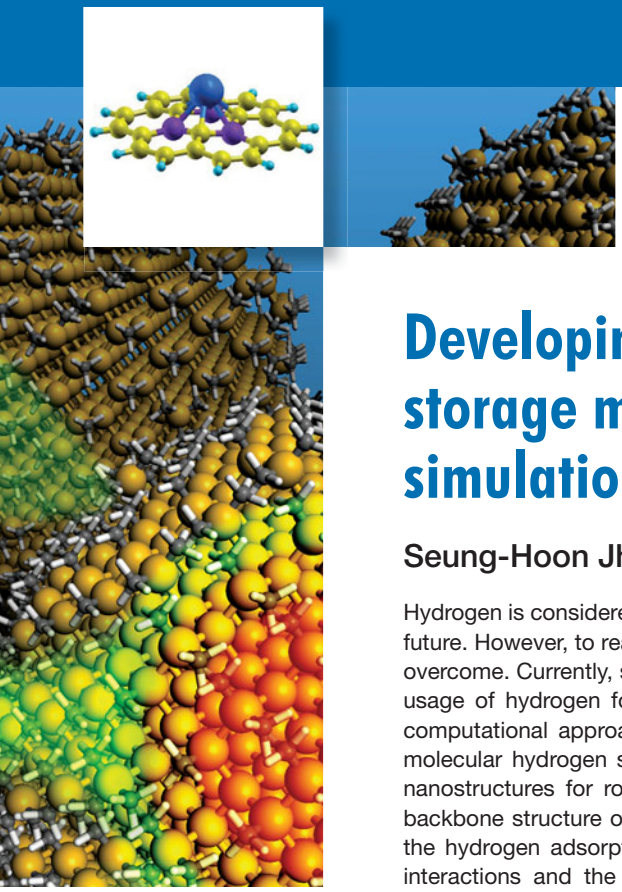


Developing high-capacity hydrogen storage materials via quantum simulations

Seung-Hoon Jhi and Jisoon Ihm

Hydrogen is considered by some to be a promising non-CO_2-emitting energy carrier for the future. However, to realize a hydrogen economy, there are several technological barriers to overcome. Currently, safe and efficient storage of hydrogen is a bottleneck in the practical usage of hydrogen for fuels. In this article, we present a review on the first-principles computational approach in designing hydrogen storage materials with an emphasis on molecular hydrogen storage in nanostructured materials. Given the limitation of pristine nanostructures for room-temperature hydrogen storage, the strategy of decorating the backbone structure of the nanostructure with transition metal atoms in order to enhance the hydrogen adsorption energy is addressed, and the interplay between the Coulomb interactions and the so-called Kubas interaction (nondissociative weak chemisorption via electron donation and back-donation channels) has been studied. The influence of electron spin on the hydrogen binding energy, problems of metal clustering and oxidation, and the structural instability that may arise during hydrogen sorption are also discussed. We address the limitations and challenges in the development of high-capacity hydrogen storage materials and provide perspectives for how computational materials design can help cope with those problems.

Introduction

Many human activities have been associated with the production, transportation, storage, and conversion of fossil fuels. Currently, hydrogen is widely regarded as an ideal energy-carrying medium without carbon dioxide emissions. Hydrogen, producible from water via electrolysis or more practically from steam reforming of hydrocarbons, is abundant, clean, and recyclable.

Despite the promise offered by hydrogen as a dispatchable fuel, a number of fundamental and technical problems must be solved before commercial-scale use of hydrogen energy can be realized.[1,2] In the field of hydrogen storage, the issues include safety, high capacity, moderate operating temperature and pressure, fast kinetics, and recyclability. Compressed hydrogen gas, liquid hydrogen, and chemical or metal hydrides are readily available forms of storage for which there exists a long research history. On the other hand, adsorbing molecular hydrogen on solid surfaces is a relatively new storage paradigm that is under active research. While many materials have been studied for room-temperature hydrogen storage, the achieved capacity is still short of the desired level for practical applications. Since typical hydrogen interactions with solid surfaces tend to be via physisorption (~5 kJ/mol) or chemisorption (>100 kJ/mol), the storage of a meaningful amount of hydrogen requires technically harsh conditions, such as cryogenic temperatures and/or high pressures on the order of several hundred bars. Exploiting metal-dihydrogen complexes that are stabilized by the so-called Kubas interaction (to be explained later) therefore represents a game changer in the pursuit of technologically viable approaches to hydrogen storage.[3]

Computation by quantum mechanical methods has proven to be very powerful to predict key physical properties of materials such as crystal structure, electronic and optical properties, transport properties, and gas adsorption kinetics. Combining quantum mechanical simulations and experimentation can dramatically improve the efficiency of developing high-capacity hydrogen storage. We first give a brief historical introduction to the use of carbon-based nanomaterials for hydrogen storage and the role of residual metal particles in hydrogen sorption in these materials. The possibility of the spillover phenomenon

Seung-Hoon Jhi, Pohang University of Science and Technology, Republic of Korea; jhish@postech.ac.kr
Jisoon Ihm, Seoul National University, Republic of Korea; jihm@snu.ac.kr
DOI: 10.1557/mrs.2011.32

© 2011 Materials Research Society
https://doi.org/10.1557/mrs.2011.32 Published online by Cambridge University Press

(dissociation and diffusion of adsorbed hydrogen on the adsorbent) is discussed as well. Next, we describe in more detail the widely used method of dispersing metal atoms in the backbone structure to enhance the hydrogen binding energy. The significance of the Kubas interaction is emphasized in this respect. Various strategies to avoid metal clustering in the process of metal decoration as well as to reduce the oxidation tendency after or during metal deposition are presented. The influence of electron spin on hydrogen binding energy and the structural instability that may arise during hydrogen sorption are also discussed.

Computational methods

Recently, first-principles quantum mechanical simulations have reached a level of sophistication that enables computational elucidation of the mechanism of the hydrogen adsorption on framework materials with high accuracy. These tools also can provide detailed quantitative information on the structure and chemistry of hydrogen storage materials. These first-principles methods tend to be either density functional theory (DFT) or wave function methods. Their accuracy depends on the basis set and the treatment of the exchange-correlation of electrons.[4–7]As in other applications of first-principles methodologies, the central algorithmic issue is to identify a sufficiently accurate approximation of the quantum mechanical exchange-correlation of electrons associated with hydrogen adsorption. In particular, physisorption of hydrogen due to medium-range van der Waals (or dispersion) interactions is poorly described by typically employed exchange-correlation density functional approximations such as the generalized gradient approximation (GGA) and the local density approximation (LDA). Care must be taken in accounting for metal–hydrogen interactions because the error from improper handling of the exchange-correlation can sometimes be significant.[8,9]

The Hartree-Fock (HF) method, a starting point for wave function methods, incorporates exact exchange interactions, but electron correlation is completely neglected. Post-HF methods, such as Møller–Plesset second order perturbation theory (MP2),[10] were devised to incorporate the correlation of electrons. Even more highly correlated methods, such as coupled cluster[11] or quantum Monte Carlo (QMC)[12] methods, are the point of reference for testing the accuracy of DFT, HF, or MP2 analyses. Hybrid functionals also have received a good bit of attention, in which Hamiltonians are based on linear combinations of HF exchange and the DFT exchange-correlation functionals.[13]

Bajdich et al.[14] carried out a comprehensive comparison among DFT, wave-function, and QMC methods, concluding that the error from GGA or LDA in DFT calculations comes mostly from the exchange functional. QMC calculations of H_2 binding on Ca^+ ion were closely reproduced by DFT calculations when the exact exchange functional plus the GGA correlation was used. Shimka et al.[15] reported an interesting study of molecular adsorption on metal surfaces; the random phase approximation (RPA) for screening built into the HF methods gives very reliable results of adsorption energies and binding sites for CO and benzene on transition metal surfaces, as compared with experiments. In the RPA, electrons are assumed to respond in a self-consistent way to the total electric potential, which is the sum of the external potential and a screening potential. Studies so far suggest two realistic solutions to account for electron exchange and correlation in association with hydrogen adsorption analyses: the pragmatic choice of exact exchange combined with GGA correlation, or a more rigorous and accurate method of exact exchange combined with RPA correlation.

We typically use plane-wave–based, first-principles methods, such as those implemented in the VASP (Vienna *ab initio* simulation package) and Quantum Espresso codes. The former is commercially available for academic licensing, while the latter is in the public domain. These codes are run on high-performance computing platforms, essential for the problem sizes of interest here. For example, we often use clusters based on Intel quad-core Xeon CPUs (2.66 GHz). Computing nodes are interconnected by either Gigabit or Infiniband switches (Infiniband provides a much faster communication between the nodes.). The computing time depends on the system size and the accuracy required for each problem. Suppose we calculate the hydrogen-binding energy in a metal-graphene complex within 1 meV or 0.1 kJ/mol accuracy. The total energy calculation of hydrogen together with the metal-graphene complex consists of two loops: a loop for self-consistent DFT calculations for a given atomic position and a loop for the relaxation of atomic position. With one node consisting of two quad-core CPUs, the first loop takes about 500 seconds, and the second loop involves 100 iterations. The total time will therefore be about 12 hours. Similar calculations are repeated for 10s of different configurations. The timeframe for a typical binding energy calculation ranges from a few days to a few weeks with this computing system.

Porous carbon nanomaterials and metal residue

Carbon-based nanomaterials, such as carbon nanotubes (CNTs) and fullerenes, have attracted a great deal of attention because they have an extremely large surface area and enhanced capillary reactions with molecules.[16,17] The sp^2-bonding between carbon atoms ensures the stability and the large surface area of these materials. These promising attributes prompted people to readily consider carbon nanomaterials for gas sensing and hydrogen storage applications. Early measurements reported overly optimistic results, wherein CNTs were found to uptake hydrogen by about 5–10 wt% (gravimetric density, namely, the usable hydrogen weight over the total storage system weight) at room temperature and moderately high pressures.[18,19] Despite these data, first-principles calculations predicted that H_2 molecular binding on bare carbon nanomaterials is very weak, with binding energies similar to those associated with van der Waals

https://doi.org/10.1557/mrs.2011.32 Published online by Cambridge University Press

interactions (~5 kJ/mol) and binding distances of about ~3.3 Å.[20–22] Later experiments consistently showed that, due to such small adsorption energies, the room temperature storage capacity of these materials is not more than 1 wt%, and that a technologically important capacity (~6 wt%) could only be reached at cryogenic temperatures. For reference, the U.S. DOE target capacity for the year 2015 is 5.5 wt% and 40 g/L (volumetric density, namely, usable hydrogen weight over the total storage system volume). Therefore, it became necessary to seek other mechanisms and structures to improve hydrogen binding on sorption materials such as hydrogen spillover,* metal dispersion, or structural/chemical modifications.[23–28]

There has been a controversy as to whether residual metal catalysts used in growing CNTs act as hydrogen sorption materials or as catalysts to drive hydrogen into the carbon nanostructures.[29,30] It was suggested that hydrogen dissociation and subsequent spillover to CNTs by metal catalysts can lead to high-capacity storage.[23,31] According to this model, the metal catalysts dissociate hydrogen molecules into H atoms, which then diffuse along the surface of activated carbon, making sp^3 bonds. The storage capacity was reported to be as high as ~3.7 wt% at 69 bar in a sample of multi-walled CNTs.[31] This intriguing phenomenon of hydrogen spillover has been regarded as an efficient method to overcome the drawback of weak molecular hydrogen adsorption and insufficient space in carbon nanomaterials. However, first-principles calculations suggested that individual hydrogen molecules would favor the gas phase over atomic chemisorptions to sp^2-bonded carbon.[32,33] On the other hand, fully hydrogenated graphene (or graphane) is stable against segregated graphene and hydrogen gas.[34] It was shown that hydrogenation of graphene can be energetically favorable when a certain amount of hydrogenation is initiated.[32] Cumulative binding of H atoms may be plausible at the boundary of the domains of pre-bound H atoms. Since the dissociation and diffusion of hydrogen involves excited transient states, it is unclear whether energetics alone can determine the feasibility of hydrogen spillover. Hydrogenation via spillover of graphene, metal organic frameworks (MOFs),** and other materials with a high surface area is still an active issue in hydrogen storage research.[35]

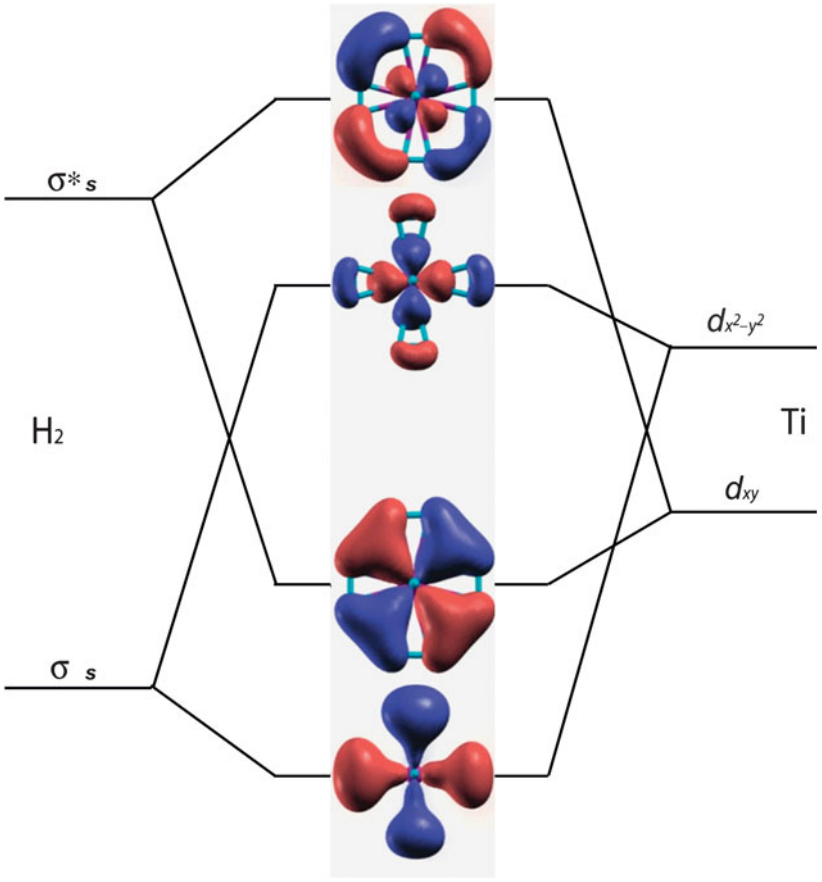


Figure 1. Hybridization diagram between H_2 and Ti under the octahedral ligand field. The 3*d* orbitals of the Ti atom are decomposed into e_g ($d_{x^2-y^2}$ and $d_{3z^2-r^2}$) and t_{2g} (d_{xy}, d_{yz}, and d_{zx}) orbitals. An isolated H_2 can have σ (bonding) and σ* (anti-bonding) *s* orbitals. The isosurfaces of the electron wave functions of the hybridized orbitals are also shown in the middle. The color of the isosurfaces denotes the sign of wave functions. This metal-dihydride complex is stabilized via the Kubas interaction (nondissociative weak chemisorption via electron donation and back-donation channels). Red denotes positive, and blue denotes negative. Adapted from Reference 39.

Metal decoration in porous materials and Kubas interactions

The interaction of H_2 with sorption materials is a key parameter that controls the desorption temperature and pressure as well as the ultimate storage capacity of a material. The desirable adsorption energy of H_2 under conditions for practical

* The hydrogen spillover refers to a dissociative and diffusive adsorption of hydrogen assisted by metal catalysts. H_2 is bound to a metal catalyst surface through a dissociative mechanism that splits the hydrogen molecule into two H atoms, and those H atoms diffuse down onto the surface of the sorption materials.

** Similar to other high-surface area materials, H_2 is bound to the constituent atoms of the MOF basically through weak van der Waals interactions. Exposed open metal sites in MOFs could serve as stronger binding centers of hydrogen. Under low temperature and high pressure, a substantial amount of H_2 gas molecules may be stored in the void volume of the MOF as well. If the spillover phenomenon should be in effect, additional storage by hydrogen atoms attached to the inner surface of the MOF would be possible.

https://doi.org/10.1557/mrs.2011.32 Published online by Cambridge University Press

applications is in the range of 20–40 kJ/mol according to equilibrium thermodynamic calculations (including vibrational contributions).[36] Since H_2 molecular attraction to sorption materials is usually through weak van der Waals interactions, the increase of binding energies to optimal values has been a major issue in designing hydrogen storage materials via computations.

Niu et al.[37] studied molecular hydrogen binding with ionized transition metals (TMs), showing that several H_2 molecules can be adsorbed on metal ions with an energy range of about 30–50 kJ/mol, but their study was not immediately applied to the hydrogen storage problem. Lochan and Head-Gordon[38] carried out a comprehensive study for other metal ions. TM ion-H_2 complexes (known as Kubas complexes) are usually stabilized by two co-existing mechanisms (**Figure 1**). An occupied H_2 σ-bonding orbital can hybridize with an unoccupied TM *d* orbital, which is called the electron donation channel. An occupied TM *d* orbital can hybridize with an unoccupied H_2 σ^*-antibonding orbital, which is called the back donation channel. Two interactions occur simultaneously in a typical Kubas complex.[3,39] A clear fingerprint of back donation is the elongation of H–H bond length to about ~0.85–0.9 Å from an equilibrium value of ~0.75 Å. Several first-principles calculations reported potential hydrogen storage that utilize TM-decorated CNTs,[26] fullerenes,[27] polymers,[28] or 3D graphene.[40] TM atoms prefer to sit on the center of aromatic carbon rings in, for example, CNT or graphene with binding energies of ~2 eV. The first H_2 adsorbed on a TM atom tends to dissociate into 2 H atoms, forming hydride, and the next 4–5 H_2 molecules are adsorbed on TM without dissociation and with a strength of about ~30–80 kJ/mol.[28] The storage capacity can reach as high as 4–8 wt% at moderate adsorption conditions, according to previously mentioned calculations.

Transition metal atoms can have unbalanced net spins, and the spin state is an important issue in understanding the binding mechanism of H_2 to the transition metal atoms.[41] The trends of the H_2 binding energy have been well-explained by the relative line up of spin-up and spin-down orbitals in comparison with crystal-field splitting.[41] When the crystal-field splitting (by ligand fields or by H_2 adsorption) becomes larger than the exchange splitting (the energy difference between spin up and down states), the system switches from a high spin state to a low spin state, resulting in a net energy gain. This indicates that, in designing hydrogen storage materials, the electron spin is a factor that should be considered and taken advantage of.

Metal clustering and oxidation

While many calculations have suggested that TM-dispersed nanomaterials could achieve high-capacity hydrogen storage at ambient conditions, experimental support for this storage paradigm has been rather scarce. Adsorption isotherm measurements indicated that 3-coordinate Ti(III) centers in a mesoporous silica backbone might hold up to five hydrogen molecules, with a binding strength of ~22 kJ/mol.[42] Phillips and Shivaram[43] reported an observation of high-capacity uptake of 2–5 H_2 per TM at room temperature in a TM-ethylene complex. However, sample preparation conditions significantly affected the metal dispersion and hydrogen binding. A potential problem that arises during metal dispersion is the aggregation of metal atoms. Sun et al. reported the possibility of clustering of metal atoms in backbone structures.[44] It was shown that Ti atoms on C_{60} are energetically unstable against clustering. Obviously, the number of available hydrogen binding sites is reduced drastically when metal clustering occurs. Furthermore, the transition metal atoms are so reactive that they can destroy the structure of backbone materials or dissociate hydrogen and other molecules. In fact, isotope-dependent temperature-programmed desorption measurements on Ti-deposited polyaniline showed a signature of Ti clustering.[45]

The tendency of metal atoms to cluster derives from the large cohesive energy of metal as compared with the binding energy of individual metal atoms to the backbone material. One possible solution to this problem is to increase the binding energy of individual metal atoms to the backbone (**Figure 2**). It was shown that B-doping in graphene increases the metal binding energy appreciably and also affects the hydrogen adsorption.[46,47] The hole doping in graphene enhances the charge transfer from

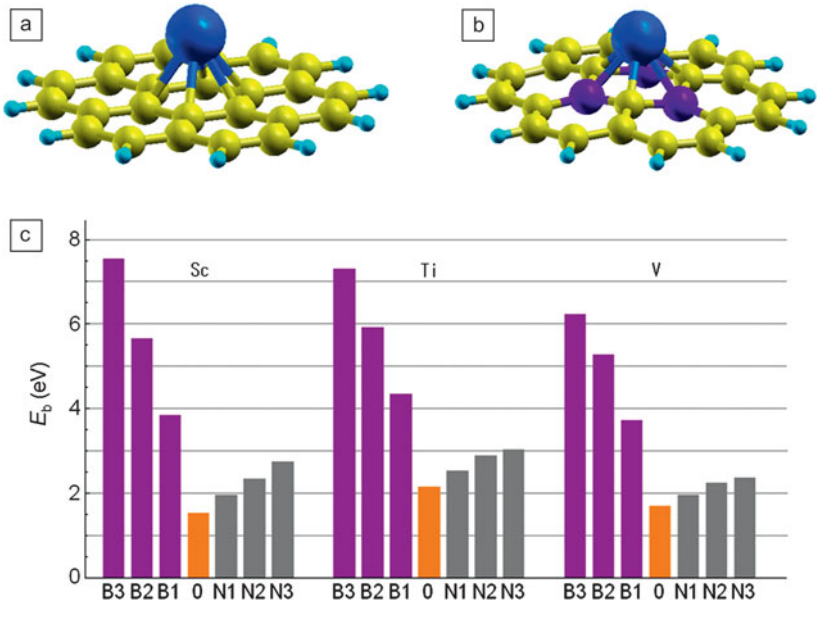


Figure 2. Atomic structure of Ti attached to (a) a pure and (b) a B-doped coronene (a polycyclic aromatic hydrocarbon, $C_{24}H_{12}$, consisting of seven benzene rings) molecule. Yellow balls, carbon; purple balls, boron; large blue balls, titanium; small light-blue balls, hydrogen. (c) Calculated binding energies E_b of transition metal atoms (Sc, Ti, and V) on boron or nitrogen-doped coronenes (1 eV = 96.5 kJ/mol). B*n* (N*n*) denotes *n* B (N) atoms in a carbon hexagon ring without forming B–B (N–N) bonding. The number 0 indicates the pristine coronene case. Adapted from Reference 46.

https://doi.org/10.1557/mrs.2011.32 Published online by Cambridge University Press

metal to graphene and changes the occupation of metal *d* orbitals.[46] Since the strength of the Kubas interaction and the number of adsorbed H_2 binding depend on the level and occupation of *d* orbitals, optimal storage materials may be designed by chemical doping and structural modification that change the binding strength and charge transfer between the transition metal and sorption materials.

Another problem in metal decoration is the oxidation of metal atoms, which will block the adsorption of H_2 to the metal. Partial hydrogenation of metal ions, which occurs at initial hydrogen binding, can suppress oxidation to a certain extent, while providing non-bonding *d* orbitals for hydrogen adsorption. Since oxygen generally contaminates the material and badly degrades the storage system, it is necessary to seal and shield the system against oxygen penetration and to also install an oxygen getter. One possible strategy to alleviate the oxidation problem is to use a metal that has less of a tendency to oxidize, such as Fe, as opposed to Ti. The advantage of Fe decoration on the framework structure has been described in the literature.[9,48] In fact, if the MOF is functionalized with OH, for example, then transition metal atoms preferentially attach to the functional groups so that metal clustering is avoided. **Figure 3** shows a schematic configuration of maximally adsorbed H_2 on a Fe-decorated, OH-functionalized MOF.[48]

Non-transition metal decoration

Non-transition metals such as Li, Na, Mg, and Ca also have been studied as hydrogen binding centers in various dispersive media.[49–55] Lochan and Head-Gordon[38] calculated, using first-principles wave function methods, hydrogen adsorption on bare ionic alkali metal atoms, Li^+, Na^+, Mg^{2+}, and Al^{3+}, and found that they hold up to six hydrogen molecules, with binding energies varying from 10–12 kJ/mol (Na^+) up to 116–350 kJ/mol (Al^{3+}). This result supports the contention that, once alkali or alkaline-earth metals can exist as bare ions in porous media, they will provide binding centers for H_2 adsorption.[56] Ca has been regarded as particularly promising in this regard because of its smaller bulk cohesive energy (~180 kJ/mol) as compared with that of TMs (~400–500 kJ/mol), implying much weaker tendency toward clustering. Ca has the added advantage that empty *d* orbitals can have the Kubas-type interaction with H_2. It was shown that each Ca ion on the CNT or fullerene holds up to six H_2 molecules, with the binding strength of ~10–20 kJ/mol.[50,51,53,57]

Chemical modifications of sorption materials also induce a noticeable change in Ca *s* and *d* orbital occupation, and it dramatically affects the hydrogen adsorption on Ca ions. An interplay between electrostatic Coulomb and Kubas interactions occurs when *s* and *d* levels of Ca on graphene are exchanged upon multiple H_2 adsorption. The first H_2 adsorption on the Ca^+ ion in pristine graphene is mostly mediated by the induced dipole and quadruple interactions. As more hydrogen molecules are adsorbed on Ca, the repulsive potential of hydrogen electrons pushes Ca *s* orbitals into a higher energy than Ca *d* orbitals so that *d* orbitals become partially occupied. When this *s-d* level reversal occurs, the Kubas-type interaction (in its broad sense, namely, at least the donation channel mentioned previously clearly exists, although

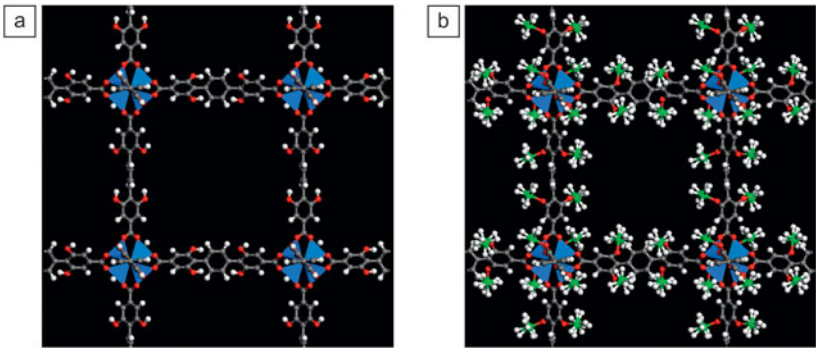


Figure 3. Proposed geometry of hydrogen adsorption on Fe-decorated, OH-functionalized metal organic framework (MOF). The junction region is shown in blue (detailed atomic structures are omitted for simplicity); the linker part (bridging organic ligands) is shown in gray; oxygen atoms are red dots; hydrogen atoms are white dots; and Fe atoms are green dots. (a) One of the MOF structures is functionalized with a hydroxyl group (OH). (b) Fe-decorated, OH-functionalized MOF with maximally adsorbed H_2 on it. H_2 gas molecules residing in the void volume at the center are not shown for visual clarity. Adapted from Reference 48.

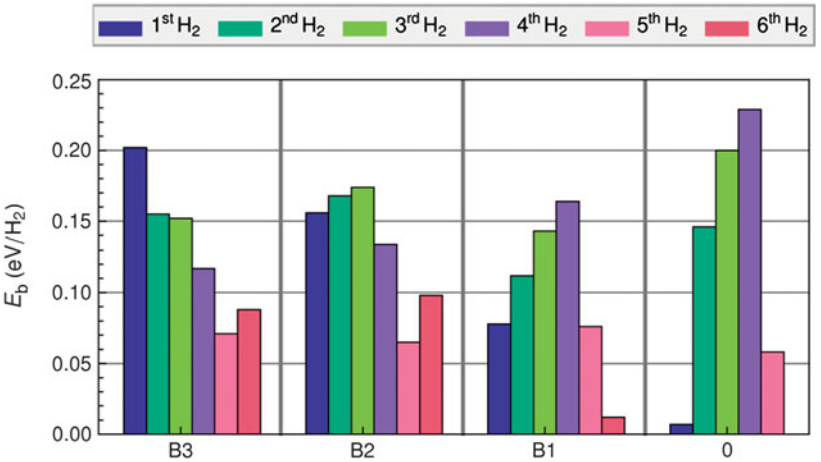


Figure 4. Consecutive H_2 binding energies (E_b) to Ca–$C_{32-x}B_x$ complexes calculated with the density functional theory method within the generalized gradient approximation (1 eV = 96.5 kJ/mol). The label in the abscissa: *n* in B*n* denotes the number of boron atoms substituting carbon atoms at a defect site. Boron doping improves the hydrogen adsorption properties in Ca-decorated graphene by enhancing the Kubas interaction (nondissociative weak chemisorption via electron donation and back-donation channels) between Ca and H_2 molecules. Adapted from Reference 51.

https://doi.org/10.1557/mrs.2011.32 Published online by Cambridge University Press

the back-donation channel may be fairly weak) provides the dominant binding energy for a stronger and more stable configuration. **Figure 4** shows the very small adsorption energy for the first H_2 and then a significant increase in subsequent adsorption energies on Ca in pristine graphene due to the onset of the Kubas interaction.

Porous frameworks and hybrid 3D structures

Computational optimization of hydrogen binding energy represents only one facet of the design process. Successful material systems also must have a large surface area and pore volume essential for high gravimetric and volumetric capacity as well as fast kinetics. Therefore, another critical question is how to sustain enough space and structural stability between individual constituents so as to utilize them as both a hydrogen sorption material and as a backbone for metal dispersion. Not only metal clustering, but also the deterioration of backbone materials, is likely to occur during cycles of hydrogen storage and release. Regarding this issue, we introduce some hybrid carbon structures considered as potential backbone materials.[40,58–64]

The sp^2-bonded carbon structures, such as CNT and graphitic nanostructures, can, in principle, have a large surface area (greater than 1000 m^2/g), but the interlayer spacing is limited to about ~3.4 Å. This is not sufficient for molecular hydrogen adsorption, diffusion, and metal dispersion. In order to overcome such structural shortcomings, hybrid structures combining different types of nanostructures have been proposed.[62] Graphite intercalated with C_{60}, CNTs, or other molecules;[59,63,64] graphene-based three-dimensional structures;[40,58] and pillared carbon materials[60,61] were considered for hydrogen storage. **Figure 5** shows the graphene-based three-dimensional structure, named covalently bonded graphene (CBG), which consists of graphene stripes interconnected by the sp^3-bonded carbon atoms at the vertices. By adjusting the pillar molecules or the width of graphene stripes that build the CBG structures, the pore size can be controlled. One immediate implication is that the hybrid nanostructures could set another pathway to achieve a maximal gravimetric and volumetric capacity for the molecular hydrogen storage. For metal-decorated covalently bonded graphene, the ideal maximum gravimetric capacity is estimated to be ~10 wt%, with a volumetric capacity of ~67 g/L when 6 H_2 molecules are adsorbed on each metal atom. These are currently only theoretically proposed structures, and their usefulness needs be confirmed by experiment.

In addition to the materials systems already discussed, there are cross-linked polymers, carbide-derived carbon, and many other porous structures.[65,66] In particular, MOFs and covalent organic frameworks have been studied extensively,[56,67–69] but a review of these materials is beyond the scope of the present article.

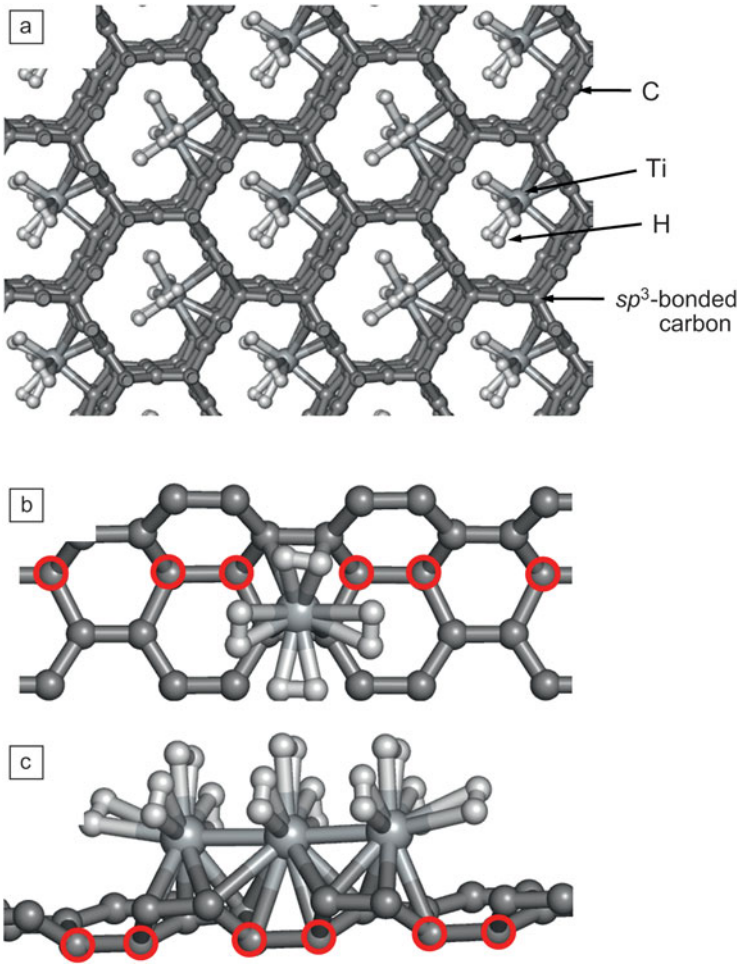


Figure 5. (a) Perspective view of the covalently bonded graphene (CBG) with Ti atoms affixed at the vertex sites and hydrogen molecules on Ti. Here each Ti adsorbs four hydrogen molecules. Enlarged side views of (b) four hydrogen molecules adsorbed on a Ti atom at the vertex and (c) 11 hydrogen molecules on the Ti trimer affixed to the vertex sites of the CBG. The red circles in (b) and (c) denote the sp^3-bonded carbon atoms. Adapted from Reference 40; see Reference 40 for more details.

Summary

We have reviewed representative materials and mechanisms for molecular hydrogen storage from the perspective of computational materials design. With the rapid increase in computational power and the development of optimized first-principles packages[4,70] incorporating improved exchange-correlation functionals such as hybrid generalized gradient approximation functionals, an accurate and fast search of realistic solid materials for hydrogen storage has become possible. Practical operating conditions require hydrogen adsorption energies of a few 10s of kJ/mol. Stable metal-dihydrogen complexes can provide a platform to achieve such intermediate adsorption strengths that lie between those of physisorption and chemisorption, and metal-decorated porous materials have been discussed as potential candidates for this. We have addressed issues and problems concerning metal-decorated nanostructures: metal clustering,

https://doi.org/10.1557/mrs.2011.32 Published online by Cambridge University Press

stability of backbone structures, oxidation, and other materials limitations such as surface areas and pore sizes.

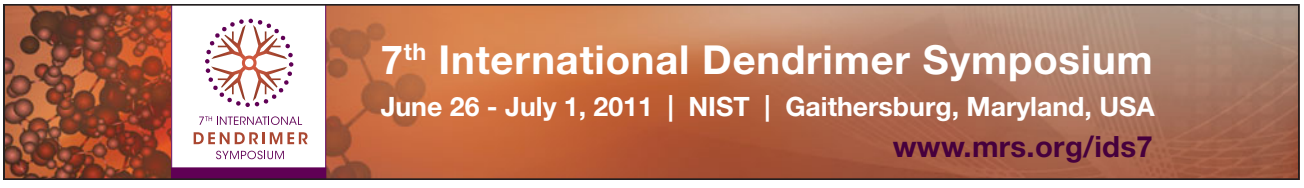
Computational design of hydrogen storage materials that can operate at ambient conditions needs to meet with two primary challenges: finding a mechanism that has the appropriate interaction strength noted previously; and providing a stable (chemically, thermally, and mechanically) porous structure that possesses a large available surface, affording interaction sites for H_2 molecules. Metal-decorated metal organic frameworks/covalent organic frameworks, high surface area heteropolar materials, graphene or graphite-related structures, bioinspired materials, and structures that exploit excited states of chemistry are among the areas that remain to be pursued in future research.

Acknowledgments

S.-H.J. was supported by the Hydrogen Energy R&D Center, one of the 21st Century Frontier R&D Programs, and also by the WCU program (No. R31-2008-000-10059-0), funded by the Ministry of Education, Science and Technology (MEST) of Korea. J.I. acknowledges the support of the Core Competence Enhancement Program (2E21580) of KIST through the Hybrid Computational Science Laboratory, the Korean Government MEST Basic Research Fund No. KRF-2006-341-C000015, and the Hanwha Chemical Co.

References

1. L. Schlapbach, A. Zuttel, *Nature* **414**, 353 (2001).
2. S. Satyapal, J. Petrovic, C. Read, G. Thomas, G. Ordaz, *Catal. Today* **120**, 246 (2007).
3. G.J. Kubas, *J. Organomet. Chem.* **635**, 37 (2001).
4. M.C. Payne, M.P. Teter, D.C. Allan, T.A. Arias, J.D. Joannopulos, *Rev. Mod. Phys.* **64**, 1045 (1992).
5. P. Geerlings, F. De Proft, W. Langenaeker, *Chem. Rev.* **103**, 1793 (2003).
6. C. Adamo, V. Barone, *J. Chem. Phys.* **110**, 6158 (1999).
7. T.H. Dunning, *J. Phys. Chem. A* **104**, 9062 (2000).
8. J. Cha, S. Lim, C.H. Choi, M.H. Cha, N. Park, *Phys. Rev. Lett.* **103**, 216102 (2009).
9. Y.H. Kim, Y.Y. Sun, W.I. Choi, J. Kang, S.B. Zhang, *Phys. Chem. Chem. Phys.* **11**, 11400 (2009).
10. M. Head-Gordon, J.A. Pople, M.J. Frisch, *Chem. Phys. Lett.* **153**, 503 (1988).
11. J. Čížek, *J. Chem. Phys.* **45**, 4256 (1966).
12. W.M.C. Foulkes, L. Mitas, R.J. Needs, G. Rajagopal, *Rev. Mod. Phys.* **73**, 33 (2001).
13. A.D. Becke, *J. Chem. Phys.* **98**, 5648 (1993).
14. M. Bajdich, F.A. Reboredo, P.R.C. Kent, *Phys. Rev. B* **82**, 081405 (2010).
15. L. Schimka, J. Harl, A. Stroppa, A. Grüneis, M. Marsman, F. Mittendorfer, G. Kresse, *Nat. Mater.* **9**, 741 (2010).
16. J. Kong, N.R. Franklin, C.W. Zhou, M.G. Chapline, S. Peng, K.J. Cho, H.J. Dai, *Science* **287**, 622 (2000).
17. J.K. Holt, H.G. Park, Y.M. Wang, M. Stadermann, A.B. Artyukhin, C.P. Grigoropoulos, A. Noy, O. Bakajin, *Science* **312**, 1034 (2006).
18. A.C. Dillon, K.M. Jones, T.A. Bekkedahl, C.H. Kiang, D.S. Bethune, M.J. Heben, *Nature* **386**, 377 (1997).
19. C. Liu, Y.Y. Fan, M. Liu, H.T. Cong, H.M. Cheng, M.S. Dresselhaus, *Science* **286**, 1127 (1999).
20. J.S. Arellano, L.M. Molina, A. Rubio, M.J. Lopez, J.A. Alonso, *J. Chem. Phys.* **117**, 2281 (2002).
21. O. Gulseren, T. Yildirim, S. Ciraci, *Phys. Rev. B* **66**, 121401 (2002).
22. Y. Okamoto, Y. Miyamoto, *J. Phys. Chem. B* **105**, 3470 (2001).
23. F.H. Yang, R.T. Yang, *Carbon* **40**, 437 (2002).
24. J. Chen, F. Wu, *Appl. Phys. A* **78**, 989 (2004).
25. S.H. Jhi, Y.K. Kwon, *Phys. Rev. B* **69**, 245407 (2004).
26. T. Yildirim, S. Ciraci, *Phys. Rev. Lett.* **94**, 175501 (2005).
27. Y.F. Zhao, Y.H. Kim, A.C. Dillon, M.J. Heben, S.B. Zhang, *Phys. Rev. Lett.* **94**, 155504 (2005).
28. H. Lee, W.I. Choi, J. Ihm, *Phys. Rev. Lett.* **97**, 056104 (2006).
29. M. Hirscher, M. Becher, M. Haluska, U. Dettlaff-Weglikowska, A. Quintel, G.S. Duesberg, Y.M. Choi, P. Downes, M. Hulman, S. Roth, I. Stepanek, P. Bernier, *Appl. Phys. A* **72**, 129 (2001).
30. P. Costa, K.S. Coleman, M.L.H. Green, *Nanotechnology* **16**, 512 (2005).
31. A. Lueking, R.T. Yang, *AIChE J.* **49**, 1556 (2003).
32. D. Stojkovic, P. Zhang, P.E. Lammert, V.H. Crespi, *Phys. Rev. B* **68**, 195406 (2003).
33. Y. Lin, F. Ding, B.I. Yakobson, *Phys. Rev. B* **78**, 041402 (2008).
34. J.O. Sofo, A.S. Chaudhari, G.D. Barber, *Phys. Rev. B* **75**, 153401 (2007).
35. Y.W. Li, R.T. Yang, *J. Am. Chem. Soc.* **128**, 726 (2006).
36. H. Lee, W.I. Choi, M.C. Nguyen, M.H. Cha, E. Moon, J. Ihm, *Phys. Rev. B* **76**, 195110 (2007).
37. J. Niu, B.K. Rao, P. Jena, *Phys. Rev. Lett.* **68**, 2277 (1992).
38. R.C. Lochan, M. Head-Gordon, *Phys. Chem. Chem. Phys.* **8**, 1357 (2006).
39. M.C. Nguyen, H. Lee, J. Ihm, *Solid State Commun.* **147**, 419 (2008).
40. N. Park, S. Hong, G. Kim, S.H. Jhi, *J. Am. Chem. Soc.* **129**, 8999 (2007).
41. Y.Y. Sun, Y.H. Kim, S.B. Zhang, *J. Am. Chem. Soc.* **129**, 12606 (2007).
42. A. Hamaed, M. Trudeau, D.M. Antonelli, *J. Am. Chem. Soc.* **130**, 6992 (2008).
43. A.B. Phillips, B.S. Shivaram, *Phys. Rev. Lett.* **100**, 105505 (2008).
44. Q. Sun, P. Jena, Q. Wang, M. Marquez, *J. Am. Chem. Soc.* **128**, 9741 (2006).
45. T.S. Kim, K.J. Kim, S.K. Jo, J. Lee, *J. Phys. Chem. B* **112**, 16431 (2008).
46. G. Kim, S.H. Jhi, N. Park, S.G. Louie, M.L. Cohen, *Phys. Rev. B* **78**, 085408 (2008).
47. Y.F. Zhao, M.T. Lusk, A.C. Dillon, M.J. Heben, S.B. Zhang, *Nano Lett.* **8**, 157 (2008).
48. M.-H. Cha, M.C. Nguyen, Y.L. Lee, J. Ihm, *J. Phys. Chem. C* **114**, 14276 (2010).
49. K.R.S. Chandrakumar, S.K. Ghosh, *Nano Lett.* **8**, 13 (2008).
50. M. Yoon, S.Y. Yang, C. Hicke, E. Wang, D. Geohegan, Z.Y. Zhang, *Phys. Rev. Lett.* **100**, 206806 (2008).
51. G. Kim, S.H. Jhi, S. Lim, N. Park, *Phys. Rev. B* **79**, 155437 (2009).
52. W. Liu, Y.H. Zhao, Y. Li, Q. Jiang, E.J. Lavernia, *J. Phys. Chem. C* **113**, 2028 (2009).
53. H. Lee, J. Ihm, M.L. Cohen, S.G. Louie, *Nano Lett.* **10**, 793 (2010).
54. K.L. Mulfort, O.K. Farha, C.L. Stern, A.A. Sarjeant, J.T. Hupp, *J. Am. Chem. Soc.* **131**, 3866 (2009).
55. A. Blomqvist, C.M. Araujo, P. Srepusharawoot, R. Ahuja, *Proc. Nat. Acad. Sci. U.S.A.* **104**, 20173 (2007).
56. M. Dinca, J.R. Long, *Angew. Chem. Int. Ed.* **47**, 6766 (2008).
57. Q. Wang, Q. Sun, P. Jena, Y. Kawazoe, *J. Chem. Theory Comput.* **5**, 374 (2009).
58. A. Bhattacharya, S. Bhattacharya, C. Majumder, G.P. Das, *J. Phys. Chem. C* **114**, 10297 (2010).
59. S.B. Chu, X.R. Hu, C.L. Du, X.B. Wu, Y.C. Dai, L.B. Hu, J.B. Deng, Y.P. Feng, *Int. J. Hydrogen Energy* **35**, 1280 (2010).
60. W.Q. Deng, X. Xu, W.A. Goddard, *Phys. Rev. Lett.* **92**, 166103 (2004).
61. G.K. Dimitrakakis, E. Tylianakis, G.E. Froudakis, *Nano Lett.* **8**, 3166 (2008).
62. G. Ferey, *Chem. Soc. Rev.* **37**, 191 (2008).
63. V. Gupta, P. Scharff, K. Risch, H. Romanus, R. Muller, *Solid State Commun.* **131**, 153 (2004).
64. S. Saito, A. Oshiyama, *Phys. Rev. B* **49**, 17413 (1994).
65. A.W.C. van den Berg, C.O. Arean, *Chem. Commun.* **668** (2008).
66. K.L. Lim, H. Kazemian, Z. Yaakob, W.R.W. Daud, *Chem. Eng. Technol.* **33**, 213 (2010).
67. N.L. Rosi, J. Eckert, M. Eddaoudi, D.T. Vodak, J. Kim, M. O'Keeffe, O.M. Yaghi, *Science* **300**, 1127 (2003).
68. Y.E. Cheon, M.P. Suh, *Angew. Chem. Int. Ed.* **48**, 2899 (2009).
69. S.S. Han, J.L. Mendoza-Cortes, W.A. Goddard, *Chem. Soc. Rev.* **38**, 1460 (2009).
70. G. Kresse, J. Furthmuller, *Phys. Rev. B* **54**, 11169 (1996). □



https://doi.org/10.1557/mrs.2011.32 Published online by Cambridge University Press